GEOPHYSICS, VOL. 87, NO. 1 (JANUARY-FEBRUARY 2022); P. WA15–WA25, 12 FIGS.
10.1190/GEO2021-0065.1

Check for updates

Downloaded 12/13/21 to 137.186.57.127. Redistribution subject to SEG license or copyright; see Terms of Use at http://library.seg.org/page/policies/terms
DOI:10.1190/geo2021-0065.1

Preserving Holocaust history: Geophysical investigations at the Ponary (Paneriai) extermination site

Alastair F. McClymont[1], Paul D. Bauman[1], Richard A. Freund[2], Jon Seligman[3], Harry M. Jol[4], Philip Reeder[5], Ken Bensimon[6], and Rokas Vengalis[7]

ABSTRACT

Holocaust mass grave sites in eastern Europe can be difficult to investigate due to a paucity of historical documentation relating to the events and because the use of traditional invasive archaeology methods raises concerns around the disturbance of the remains of Jewish people. When combined with other lines of evidence, including historic photos and eyewitness testimony, noninvasive geophysical methods help to effectively identify and demarcate buried features at Holocaust sites, limiting unnecessary excavations. Between 1941 and 1944, as many as 100,000 people were murdered at the Ponary (Paneriai) extermination site in Lithuania, but many critical details of the site layout during this period are still to be resolved, including the location of some of the mass graves and confirmation of an escape tunnel that was used by slave laborers to escape captivity and certain death at the site. At Ponary, a combination of electrical resistivity tomography (ERT) profiling, limited ground-penetrating radar data, and bare-earth elevation data (from a light and distance ranging data set) was used to confirm the location of a large unmarked mass grave with a diameter of approximately 25 m and depth of approximately 4 m. Additional ERT profiling at a second location imaged the entrance to an escape tunnel previously uncovered by an archaeological excavation in 2004, and it detected an approximately 5 m section of the continuation of the tunnel, approximately 33 m away from the tunnel entrance. The geophysical results are supported by evidence from limited archaeological excavations, historical photographs, eyewitness descriptions of the site layout, and testimonies from the few survivors who managed to escape Ponary.

INTRODUCTION

The reconstruction of historical events from the Holocaust is important, not only to provide closure to the families of victims and those directly connected to the violence that took place, but also to educate the general populace today and help prevent future genocides. This is especially important at a time when there are few survivors of the Holocaust left to share their experiences and while Holocaust awareness among the general public may be diminishing (Arsenault, 2019; Ramgopal, 2020). Confirming Holocaust history can be challenging, especially when conflicting accounts from eyewitness testimonies exist and after many years have passed since the events. This is a particular problem in eastern Europe, where Soviet governance and international isolation until the early 1990s inhibited research of Holocaust sites. Although in-depth forensic investigations of mass grave sites were completed by Soviet investigators at select sites after the war, systematic archaeological investigations of Holocaust sites could only begin in earnest after the demise of the Soviet Union, some 50 years after the end of World War II (e.g., van der Laarse, 2013; Sturdy Colls, 2015a; Freund,

Manuscript received by the Editor 4 February 2021; revised manuscript received 11 June 2021; published ahead of production 23 September 2021; published online 12 November 2021.
[1]BGC Engineering Inc., Calgary, Alberta T2E7W6, Canada. E-mail: amcclymont@bgcengineering.ca (corresponding author); pbauman@bgcengineering.ca.
[2]Christopher Newport University, Newport News, Virginia 23606, USA. E-mail: richard.freund@cnu.edu.
[3]Israel Antiquities Authority, Jerusalem 91004, Israel. E-mail: seligman.jon@gmail.com.
[4]University of Wisconsin–Eau Claire, Eau Claire, Wisconsin 54702, USA. E-mail: jolhm@uwec.edu.
[5]Duquesne University, Pittsburgh, Pennsylvania 15282, USA. E-mail: reederp@duq.edu.
[6]KMB Architects, Olympia, Washington 98501, USA. E-mail: kenbensimon@me.com.
[7]Lithuanian Institute of History, Vilnius 01108, Lithuania. E-mail: rokasven@gmail.com.
© 2022 Society of Exploration Geophysicists. All rights reserved.

Downloaded 12/13/21 to 137.186.57.127. Redistribution subject to SEG license or copyright; see Terms of Use at http://library.seg.org/page/policies/terms
DOI:10.1190/geo2021-0065.1

2019). In Lithuania, many sites where mass graves are rumored to exist have either been disturbed by subsequent development or have been altered by natural processes, including erosion and growth of new vegetation. Archaeological investigations of Holocaust sites are further complicated by sensitivities from local and international Jewish communities around disturbing human remains (e.g., Sturdy Colls, 2015b), and concerns around the exhumation of human remains after conflict or human rights abuses are not just limited to Holocaust sites (see Renshaw [2013] for a good summary of these issues).

Between 1941 and 1944, as many as 100,000 people (Tomkiewicz, 2008; Chan, 2019; as translated from Soviet Extraordinary State Commission reports from USHMM, 1995; Seligman et al., 2020) were exterminated at a single site within the Ponary forest (Ponary in English and Polish, Ponar in Yiddish, and Paneriai in Lithuanian), situated approximately 10 km southwest of Vilnius, Lithuania (Figure 1; Vilna in Yiddish; Wilno in Polish). Shortly after liberating Ponary, the Soviets undertook limited forensic examinations at the site, interviewing eyewitnesses and documenting the condition of the graves (USHMM, 1995). The comprehensive details within these reports were largely inaccessible until the collapse of the Soviet Union in the early 1990s. Investigations of the site were discouraged for most of the postwar Soviet era, and scant memorials were sanctioned by the Soviet government (Seligman et al., 2020).

Because of sensitivities related to disturbing remains and the difficulties in obtaining excavation permits, noninvasive geophysical methods have recently become an important tool for investigating Holocaust mass grave sites (e.g., Sturdy Colls, 2015a; Burds et al., 2018; Freund, 2019; Bauman et al., 2020; Rozycki et al., 2020). Geophysical methods have been used for forensic investigations of grave sites, including in cemeteries (e.g., Jones, 2008), for clandestine individual graves (e.g., Powell, 2004), and mass graves not related to the Holocaust (e.g., from the 1921 Tulsa Race Massacre [Hammerstedt and Regner, 2019] and the violent unrest in Cyprus in the 1960s and 1970s [Abate et al., 2019]). Because of their capability to noninvasively map objects and structures buried within soil and sediments, geophysical methods are an important technique in forensic investigations of sensitive grave sites where excavations are prohibited.

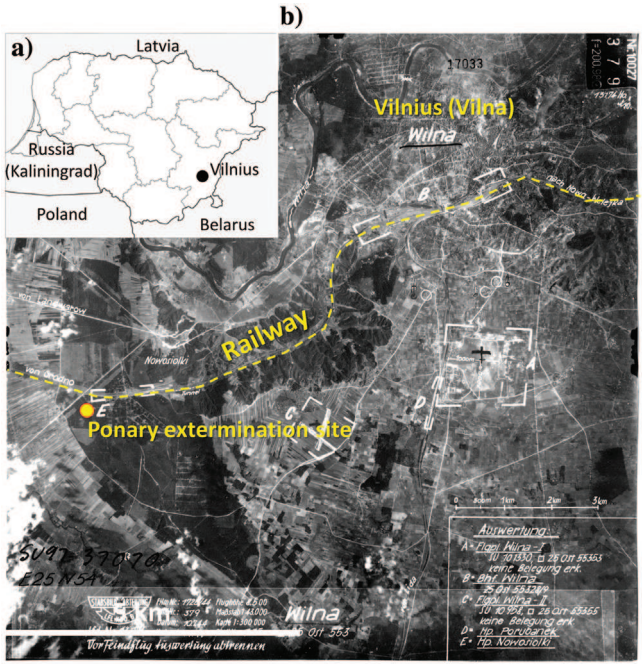


Figure 1. Study location in context of the (a) map of Lithuania and (b) map of Vilnius region, as photographed by a Luftwaffe reconnaissance flight in July 1944, annotated with the location of the railway that connected Vilnius to the Ponary extermination site. Aerial photo obtained from NARA, photo ID RG 373: DT/TM-5, Wilna, #17033 (12 × 12 in. aerial print), dated possibly 10 July 1944.

Most geophysical forensic investigations have relied on ground-penetrating radar (GPR) to delineate grave sites (e.g., Bevan, 1991; Schultz, 2012; Barone et al., 2016), largely because GPR can resolve small targets on the order of individual graves and because GPR systems have become portable and relatively easy to use. Cheetham (2005) and Jones (2008) demonstrate how geophysical methods alternative to GPR can be used for identifying graves, including earth resistivity, electromagnetic terrain conductivity, and magnetic gradiometer surveys.

Electrical resistivity tomography (ERT) is seldom used in forensic investigations, usually because individual graves may be too small to resolve using the method and because electrical resistivity contrasts are often not large enough between the material within a grave and the surrounding native soil. At the Ponary extermination site, the buried remains of mass graves are expected to be found within the unsaturated sandy sediments that blanket the site. Although these subsurface conditions are suitable for GPR surveys, they also offer an ideal opportunity to test the efficacy of the ERT technique because targets can be distinguished spatially and with depth from relatively high resistivity background material.

Until recently documentation of the history and physical arrangement of the Ponary extermination site was limited to the Soviet Extraordinary State Commission reports, survivor testimonies, and a few eyewitness reports (e.g., the accounts of local Polish journalist, Kazimierz Sakowicz; Sakowicz, 2005). Consequently, subsurface information is vital to help confirm the physical layout of the Ponary extermination site during its operation between 1941 and 1944. At the request of the Vilna Gaon State Jewish Museum in Lithuania, and in preparation for the construction of a proposed new visitor center, in 2016 a geophysical investigation was undertaken to help map subsurface evidence of what remained of the Ponary extermination site. Before undertaking this work, we consulted extensively with representatives of the Lithuanian Jewish Community and with the Vilna Gaon State Jewish Museum about how to minimize impacts to the site, and how to disseminate the results of our study. The families of those who survived or were killed at Ponary were invited to contact our research team so that we could notify them of our findings, and many were able to share anecdotal descriptions of survivor stories that assisted with our research. The 2016 investigation was also aided by the recent release from the United States National Archives and Records Administration (NARA) of German and Soviet aerial photos that covered the site in the months before and after occupation of this area by the Soviet Red Army in July 1944.

The two primary objectives of the 2016 survey were (1) to locate and map a suspected unmarked mass grave and (2) to map any remains of a tunnel used during a 1944 escape from the camp. This paper describes the geophysical field methodology, the procedures used to analyze the geophysical data, and it places the results in context with available archaeological and historical information.

Downloaded 12/13/21 to 137.186.57.127. Redistribution subject to SEG license or copyright; see Terms of Use at http://library.seg.org/page/policies/terms
DOI:10.1190/geo2021-0065.1

HISTORICAL BACKGROUND

Prior to Nazi Germany's invasion in June 1941, Soviet-occupied Lithuania was home to a Jewish community of more than 200,000 people, or as much as 10% of Lithuania's total population at the time (Snyder, 2010; USHMM, 2020). Some of the region's Jewish population arrived after 1939, fleeing violence and persecution largely from other areas of Nazi-occupied Poland. Under Nazi rule, between 1941 and 1944, as much as 95% of the Jewish population in Lithuania's postwar boundaries (Bubnys, 2004) was massacred by German and Lithuanian killing squads. The killing squads comprised the Nazi SS Einsatzgruppe A and B units, who directed local Lithuanian auxiliary policemen (Snyder, 2010; Seligman et al., 2020). Most of the victims at Ponary were Jews, brought from Lithuania's newly reinstated capital city, Vilnius, and surrounding communities by truck, train, or forced march. Tomkiewicz (2008) estimates that the number killed at Ponary included 72,000 Jews from the area surrounding Vilnius, between 15,000 and 20,000 Poles, 5000 Soviet prisoners of war (POWs), 1000 Russians and Lithuanians, and 40 Roma people.

Piecing together the scant historical sources yields some information on the physical layout of Ponary and how the killings took place (Seligman et al., 2020). At Ponary, a series of seven to nine circular pits, originally intended for fuel storage by the Soviets, were used as mass graves (Seligman et al., 2020). The circular pits were between 12 and 32 m in diameter and were excavated to depths of between 5 and 8 m within the native loose sand. To shore up the sides of some of the pits, stone walls were constructed (Vengalis, 2016). Linear trenches were excavated between the pits, which were likely intended for the installation of pipes. These trenches also served as conduits to direct the thousands of victims from the gates of the extermination site toward the pits. The installation of fuel tanks was never completed because, in June 1941, German forces occupied the area as part of their invasion of the Soviet Union. Instead, the pits were used to bury the thousands of victims who were shot and killed at Ponary between July 1941 and July 1944.

In an attempt to erase evidence of the atrocities at Ponary (as occurred at other extermination sites across Nazi-occupied eastern Europe), between December 1943 and April 1944, a contingent of 80 enslaved Jews and Soviet POWs was used to exhume bodies from the pits and burn the remains. This action was part of official Nazi policy (Sonderaktion 1005), and the slave workers were called Leichenkommando or "corpse units." The tasks of the Leichenkommando were to exhume bodies from the graves (burial pits), burn the bodies on wooden pyres, and then distribute the ash mixed with sand around the site (Seligman et al., 2020). At night, the 80 members of the Leichenkommando were imprisoned within one of the circular pits that had not been used as a mass grave (Leichenkommando detention pit; pit 6 shown in Figure 2). In a desperate attempt to escape the prison camp, between January and April 1944, members of the Leichenkommando excavated a tunnel from under the stone-lined detention pit. A mass escape was attempted through the tunnel on the evening of 15 April 1944. After the first group of prisoners exited the tunnel, German guards were alerted. Those who did not make it out of the tunnel and beyond the barbed-wire fence surrounding the camp were likely killed during or shortly after the escape attempt.

Based on survivor testimony, 12 prisoners are thought to have escaped through the tunnel and evaded capture, but only 11 survived until the end of the war (testimony of Yuri Farber in Ehrenburg and Grossman, 1986). Aside from stories told among the survivors and recorded for Claude Lanzmann's *Shoah* collection of interviews (USHMM, 1979), the tunnel, and the story of the escape, were largely undocumented until archaeological excavations uncovered the entrance to the tunnel in 2004 (Urbanavičius, 2004). The report of Urbanavičius (2004) stated an intention to conduct further studies to find the continuation of the tunnel beyond the stone wall of the detention pit. However, since the uncovering of the tunnel entrance and subsequent reburial in 2004, no further archaeological excavations have been undertaken. Remarkably, no memorial stone or signage was placed at the site to indicate the location of the rediscovered tunnel entrance. Only limited archaeological investigations have been completed at Ponary since 2004. Vengalis (2016) completed geophysical investigations around the unmarked mass grave and the escape tunnel, the results of which will be discussed in context with our 2016 geophysical investigation.

GEOPHYSICAL SURVEY AND METHODOLOGIES

The 2016 geophysical survey was undertaken at Ponary over 10 days during the period 8 June 2016 to 30 June 2016. Two sites were targeted (1) an area in the southwest corner of the site, where a mass grave was suspected but had not been identified or memorialized, and (2) the suspected location of the escape tunnel, in and outside the former Leichenkommando detention pit (pit 6 in Figure 2).

Two complementary geophysical methods were tested for the survey: ERT and GPR. Both methods are noninvasive techniques in that they can image any changes or anomalies in the shallow subsurface without actually altering the ground. As such, geophysical techniques are particularly valuable in investigations of Holocaust grave sites because there is no risk that the human remains will be disturbed.

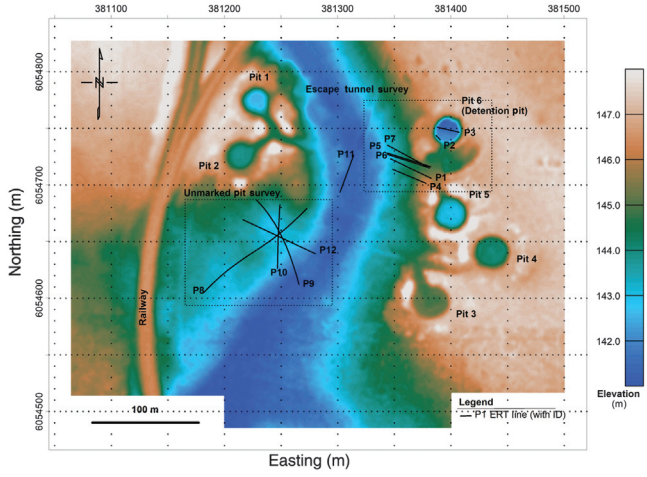


Figure 2. Ponary site location map, showing the locations of the six pits, officially memorialized at the time of the study, and the locations of the 12 ERT profiles acquired within the two main investigation areas. The background color-shaded map is the high-resolution LiDAR imagery measured in 2015. The elevated railway line on the western side of the site was constructed after World War II. The dark-blue channel through the center of the site is a paleodrainage feature.

Downloaded 12/13/21 to 137.186.57.127. Redistribution subject to SEG license or copyright; see Terms of Use at http://library.seg.org/page/policies/terms
DOI:10.1190/geo2021-0065.1

ERT methodology

The ERT technique measures changes in the electrical resistivity of the subsurface with depth beneath a profile. It is widely used in environmental and engineering studies, and it has been applied to some archaeological and forensic investigations (Noel and Xu, 1991; Fenning and Donnelly, 2003). Subsurface resistivity changes as a function of porosity, mineralogy, and the salinity of any pore water within the geologic materials (soil, sediment, or rock). In general, finer-grained geologic materials will have lower electrical resistivities relative to coarser-grained materials. Similarly, given the same material type, the electrical resistivity will change depending on the degree of consolidation or compaction of the material. As such, the ERT method is useful for distinguishing recently excavated ground that has been refilled (e.g., a grave site) from undisturbed native material. Whether the excavated ground will exhibit higher or lower resistivities relative to the surrounding material will depend on the pore-water salinity and the degree of saturation of the material, but, most importantly, the electrical resistivity of the material will be changed.

In addition to resistivity, the material chargeability (that is, the ability of the material to store electrical charge) can also be measured from an ERT survey by using the principles of induced polarization (IP) (Dahlin et al., 2002). The chargeability of the material can be determined by measuring the time it takes for the applied electrical charge to dissipate in a volume of material. Zones of high chargeability are often associated with buried metal objects. Consequently, an ERT survey configured to measure the IP response of the material can also serve as a means to detect metal artifacts buried beneath the profile. Although IP measurements indicated potential buried metal objects under some of the ERT survey lines, none of these objects were of a significant size or at a depth that would suggest they are potential artifacts from the World War II period. Metal debris dating from more recent times was found littered across the site, including drink cans and small auto parts.

All of the ERT profiles were acquired using an ABEM Terrameter LS multichannel resistivity system. At the heart of the system is a transmitter powered by a 12 V battery (equivalent to a car battery). Electrodes are inserted into the ground at uniform intervals and connected to the transmitter unit via a multicore cable. For each individual measurement, electrical current is sent to a pair of current injection electrodes (A and B), and the resulting voltage is measured on a pair of separate reception electrodes (called M and N, by convention). By varying the locations and the distances between the electrodes, the electrical resistance of the material can be measured over different depths and at distinct locations along the profile. All of the ERT profiles acquired at the site used an expanded gradient acquisition sequence, to optimize the lateral and vertical resolution of targets. Unlike traditional Schlumberger- and Wenner-type arrays, multiple-gradient arrays of this type are more efficient to collect with multichannel systems, and they have a lower sensitivity to noise than dipole-dipole arrays (Dahlin and Zhou, 2004, 2006).

The resistance measurements can be converted to apparent resistivities by applying a geometric factor that accounts for the varying electrode configurations and consequently different volumes of soil that have been measured. Data processing included removal of any negative values and obvious outliers. All ERT data were processed using RES2DINV tomographic "inversion" software, which iteratively calculates the 2D (or cross-section) model of the ground that best fits the data that have been measured (Loke and Barker, 1996). This is a process borrowed from medical imaging techniques — instead of a magnetic resonance imaging scan showing changes in brain density, the ERT method yields a cross section showing changes in the soil resistivity. All ERT inversions were calculated using L2-norm smoothness constraints on the data and the model, and model cell widths were set to equal half the minimum electrode spacing. For each inverted profile, convergence was reached after no more than five iterations and root-mean-square errors were in the range of 3%–8%.

GPR methodology

Like ERT, the GPR method provides an image of the subsurface beneath a profile. The technique involves transmitting repeating electromagnetic pulses (in the FM frequency band) from an antenna in contact with the ground, and then recording the pulses that have been reflected off subsurface layers and buried objects, and then returned to a receiving antenna. Similar to an ultrasound image, a GPR scan will produce a fuzzy picture of any structures in the soil, extending to a few meters below the ground surface. We acquired GPR data using two systems: (1) a ruggedized Groundradar UltraGPR system that looks essentially like a snake being pulled along the ground and (2) a Sensors & Software pulseEKKO system that has antennae shielded within a rigid case. The UltraGPR emitted a relatively low electromagnetic frequency of close to 80 MHz, providing a lower resolution image of targets up to 20 m below the ground surface. UltraGPR data were acquired with the antennas in an inline configuration and a separation between antenna midpoints of approximately 2 m. The positions were obtained in real time using a coupled global positioning system (GPS), and trace positions were subsequently interpolated to intervals of 0.25 m. In contrast, the pulseEKKO system used antennas with a nominal antenna frequency of 225 MHz, and data were collected along a grid in step mode, enabling higher resolution of subsurface features but limited to imaging depths shallower than the UltraGPR.

Processing of the UltraGPR data included (1) assignment of GPS coordinates to traces, (2) a time-zero correction, (3) dewow filtering, (4) application of a gain function, (5) band-pass frequency filtering, (6) interpolation of traces to cross sections with a uniform grid spacing of 0.5 m, and (7) topographic correction of the profiles. Topographic corrections were performed using a uniform velocity of 0.12 m/ns, which was estimated based on the normal moveout of subsurface diffraction patterns. Basic processing was performed on the 2016 PulseEKKO grid data, including (1) a time-zero correction, (2) dewow filtering, (3) automatic gain control, (4) trace stacking (horizontal averaging), and (5) point stacking (running average).

Survey positioning

The ERT and GPR surveys were conducted along profiles across select areas of the site (the ERT line positions shown in Figure 2). The positions of these lines were measured using handheld Trimble GeoXH GPS units and with a total station (or laser theodolite). A ground-based bare-earth light and distance ranging (LiDAR) data set of digital elevations covering most of the Ponary extermination site was undertaken in 2015, and it was provided for use in this study (Vengalis, 2016). This digital elevation model was used to correct the geophysical model cross sections for variations in the surface topography. A commercial-grade unmanned aerial vehicle

Downloaded 12/13/21 to 137.186.57.127. Redistribution subject to SEG license or copyright; see Terms of Use at http://library.seg.org/page/policies/terms
DOI:10.1190/geo2021-0065.1

(DJI Phantom 4) was also used to capture aerial images of the site, although this was of limited use due to the dense cover of trees that obscured views of the ground from above the tree canopy. All maps displayed in the figures of this paper are plotted in the WGS84/UTM Zone 35N coordinate system, with the positional coordinates shown in terms of meters east and north relative to a fixed point (eastings and northings).

UNMARKED PIT SURVEY — RESULTS AND DISCUSSION

A collection of eight historical air photos was obtained from the United States NARA and used to assess the layout of Ponary (Seligman et al., 2020), as it was in the months before and after liberation of the site in 1944. These photos were taken during German or Soviet reconnaissance flights over Ponary and date between 14 May 1944 and, potentially, as late as 14 October 1944, after the Soviets had liberated the site. These photos were georeferenced using common landmarks that are present in contemporary imagery and are also visible in the 1944 photos. In most of the photos, an area in the southwest corner of the site of light-colored disturbed ground is clearly distinguished from other vegetated areas (the "unmarked pit survey," shown in Figure 3). Within this area, a circular feature is apparent that is of similar size to the six other circular pits previously demarcated at Ponary (approximately 20–30 m in diameter).

To verify the nature of this feature, and to map its precise location on the ground, we acquired an initial 120 m-long ERT profile, oriented southwest to northeast across this feature (P8 in Figures 2 and 3). This profile used a minimum electrode spacing of 1 m, providing a reliable depth of investigation of up to 10 m below the ground surface (mbgs). In addition to the ERT, several GPR profiles were collected across this area, including a line parallel to ERT profile P8, which is shown as the gray-shaded image in Figure 4a (location shown as the yellow line in Figure 5). On this GPR line as well as on others, a prominent steeply dipping reflection was observed (between the distances of 90 and 100 m on the cross section shown in Figure 4a and 4b). Although sometimes useful, as in this instance, the GPR survey cross sections were also overprinted with reflections from aboveground trees, making it difficult to distinctly distinguish the subsurface features (see the left- to right-dipping reflection visible on the left side of Figure 4a and 4b). As such, ERT was used as the primary geophysical investigation method. An earlier GPR investigation by Vengalis (2016), using a GPR system with a nominal antenna frequency of 300 MHz, revealed, in cross section, truncations to sedimentary layers that appeared to coincide with the circular boundary of the pit shown in the 1944 aerial photo. The results of the Vengalis (2016) survey were not available until after completion of the 2016 ERT and GPR survey.

A subsequent GPR survey was completed over the area of the pit delineated by the ERT lines, using the pulseEKKO system with shielded (to block scattering from the trees) and higher frequency 225 MHz antennas. The 225 MHz data were acquired on a

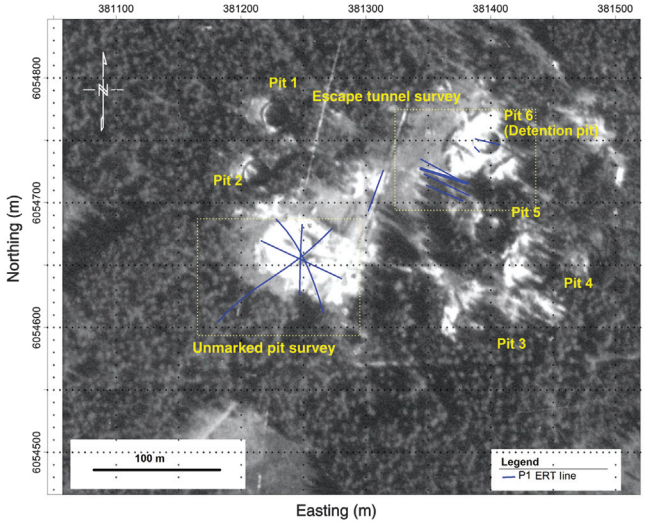


Figure 3. The same map area as shown in Figure 2 except with a georeferenced historical aerial photo taken in September 1944 at least two months after Soviet forces occupied the Ponary extermination site. Georeferencing was done by the authors in 2015. The imagery is from NARA, photo ID RG 373: GX929B SG, exp. 238 (12 × 12 in. print), dated 17 September 1944 (scale 1:13,000).

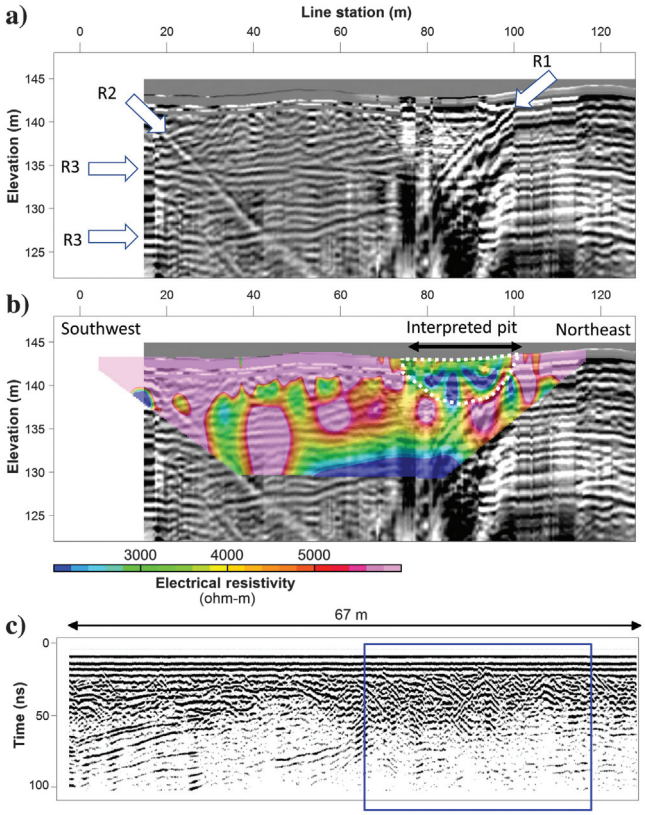


Figure 4. (a) A processed GPR cross section (grayscale image) from the 80 MHz UltraGPR system, acquired across the unmarked pit, (b) the same GPR cross section shown in (a) but overlaid with the semitransparent resistivity cross section (the color-shaded image) for ERT profile P8 (the location is shown in Figure 2), and (c) an example GPR section from the 2016 PulseEKKO GPR survey, where the blue box outlines the portion of the GPR line that crosses the unmarked pit identified from the ERT data. The annotated arrows in (a) point to an interpreted subsurface reflection "R1" coinciding with the edge of the unmarked pit, an above-ground reflection "R2," likely from trees, and two reflections, "R3," from layering within the sandy sediments surrounding the pit.

Downloaded 12/13/21 to 137.186.57.127. Redistribution subject to SEG license or copyright; see Terms of Use at http://library.seg.org/page/policies/terms
DOI:10.1190/geo2021-0065.1

40 × 40 m grid (0.25 m inline spacing; 1.0 m crossline spacing) approximately centered over the circular area of the pit defined by the ERT survey (the location is not shown in Figure 5). The circular area of the pit did correlate with a subtle change in the pattern of the reflections (Figure 4c), and it revealed similar truncated sedimentary horizons as observed by Vengalis (2016), but scattering of the radar waves from shallowly buried objects within the pit made it difficult to distinguish the boundaries of the pit accurately.

In Figure 4b, the resistivity data are plotted as a semitransparent color-shaded grid on top of the gray-shaded GPR data. The pink colors show layers and zones of relatively high resistivity sediment that we interpret as dry sands and soil with a very low clay content. The loose, dry sandy sediment is evident across most of the site. Because of these sandy soils, it would have been relatively easy to excavate pits for the proposed fuel storage tanks but more difficult to shore up the walls of the excavation — hence why some of the pits had stone wall foundations. The blue colors in Figure 4b show where the lowest resistivities were measured, including the shallow zone that extends over a distance of approximately 25 m that is interpreted to be an infilled pit.

Having identified this low-resistivity anomaly, an additional three ERT lines were centered over the feature. When plotted in 3D, the four resistivity cross sections define a circular pit feature with a diameter of 25 m and a depth of approximately 4 m (Figure 6). Closer scrutiny of the high-resolution LiDAR topographic elevation contours shows that the pit is also characterized by a very subtle circular depression that is distinct from neighboring natural drainage features (the green to brown colors in Figure 5). As shown from the photos in Figure 7, without the 1944 Luftwaffe photo, the ERT data or the LiDAR topography, the area of the mass grave would be indistinguishable from the surrounding forest. In fact, ERT profile P8 was originally located to traverse a small depression that was assumed to be a potential pit (marked as the "erosional drainage feature" in Figure 5). The ERT model for line P8 showed that this natural depression was underlain by a relatively homogeneous and undisturbed layer of dry sand, ruling out the possibility that it was associated with a mass grave (note the continuous pink layer that occurs at shallow depths between line distances of 0 and 70 m in Figure 4b).

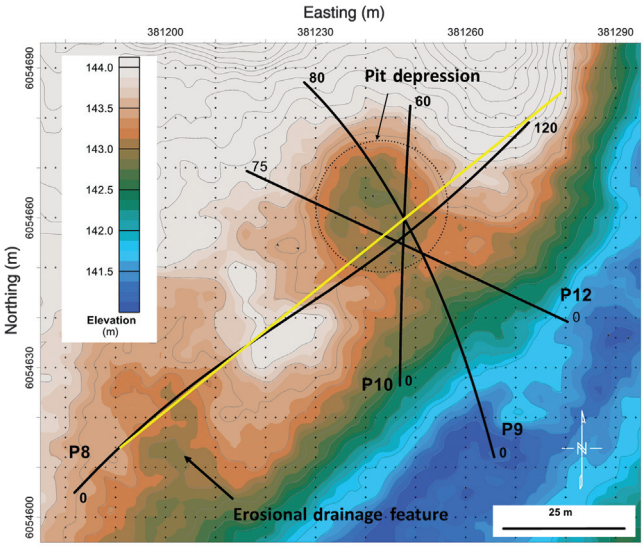


Figure 5. Map showing the layout of the unmarked pit survey and the interpreted edges of the circular pit. The circular pit is apparent as a subtle depression visible in the color-shaded LiDAR elevation data (the green to brown colors). The black lines are the ERT profiles with annotated line distances (in meters), and the yellow line shows one of the GPR profiles for the cross section shown in Figure 4a and 4b.

Although the material filling the pit exhibits much lower resistivities than the surrounding unsaturated sands, we cannot ascertain the composition of the material from the measured resistivities alone, except to infer that it is likely finer grained and/or has a higher moisture content than the surrounding dry sand. Based on the various testimonies from the surviving Leichenkommando, who described exhuming and burning bodies at the site, the pit may contain ash mobilized from the burning areas. Alternatively, records translated from the Soviet Extraordinary State Commission's forensic investigation at Ponary describe the exhumation of at least 515 bodies, suggesting that some unburned bodies remained in some of the graves after the site was liberated in 1944 (Chan, 2019).

ESCAPE TUNNEL SURVEY — RESULTS AND DISCUSSION

Our geophysical investigation of the escape tunnel relied on the findings of the Urbanavičius report of the 2004 archaeological excavations in and around the detention pit. Although the detention pit is clearly visible on the available 1944 aerial photos taken by German Luftwaffe flights (e.g., as shown in Figure 3), the photos are of too low resolution to recover details of structures inside and around the pit, including structures that may be related to the escape tunnel.

Background information from the 2004 archaeological excavation

In addition to uncovering remains of the prison bunker used by the 80 slave laborers within the detention pit, the 2004 Urbanavičius excavation uncovered a rectangular wooden frame that served as the entrance portal to the escape tunnel, and a section of the tunnel between the portal and the walls of the pit (see the excavation report photo shown in Figure 8a). The rectangular portal was uncovered in

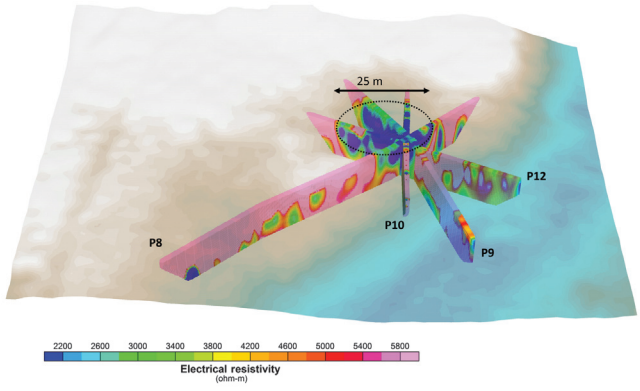


Figure 6. A 3D rendering of resistivity cross sections from the four ERT profiles acquired across the unmarked pit. The colored surface defining the high-resolution LiDAR elevation data is plotted as a semitransparent overlay. The viewing direction is to the north. The line names are annotated, and the locations are shown in Figure 5.

Downloaded 12/13/21 to 137.186.57.127. Redistribution subject to SEG license or copyright; see Terms of Use at http://library.seg.org/page/policies/terms
DOI:10.1190/geo2021-0065.1

the southwest quadrant of the detention pit at a depth of 70 cm beneath the floor of the 2004 level of the pit. The rectangle measured 80 × 95 cm and, based on the plan map shown in the excavation report, the closest side was located 1.9 m from the edge of the stone wall lining the pit (Urbanavičius, 2004). In Figure 8a, a large rock is shown within the center of the rectangle, which Urbanavičius inferred was a construction stone from the wall of the pit and left sometime after the escape of 15 April 1944.

Beneath the rectangular portal, the wooden support structure of the tunnel was also found, which was composed of a combination of vertical wooden rods (4 × 4 cm in thickness) and cut trunks and branches of pine trees (approximately 5–8 cm thick). The vertical supports had an average spacing of approximately 70 cm, whereas the slats forming the roof of the tunnel were spaced between 10 and 15 cm apart. The report noted that the tunnel support structure narrowed toward the base of the tunnel, where the vertical supports were not fastened and had been deformed by the pressure of the surrounding sand. Although the exposed tunnel was deformed in places, Urbanavičius noted in the report that "the data of the investigations do not deny the previously available knowledge that the tunnel had a size 65 × 55 cm." Based on our interpretation of the report and the accompanying photos, the tunnel structure close to the entrance was intact, but it was filled in with sand.

Remarkably, a two-core insulated wire was found leading into the tunnel, and approximately 20 batteries that may have been used as a power supply through the wire. Testimony from survivor Itzak Dugim describes the use of this wire for powering a lightbulb that was used to illuminate the tunnel and to send a signal to the tunnel diggers to evacuate in the event of an emergency (USHMM, 1979).

Geophysical survey of the tunnel entrance

To evaluate whether ERT could detect the buried tunnel structure, an 8 m-long ERT line was centered over the tunnel location, as documented in the plan drawing from Urbanavičius (2004; photo of the ERT line shown in Figure 8b). The location of this line (P2) and other lines used for the escape tunnel geophysical survey are shown in Figure 9. The ERT lines have been numbered in the order that they were acquired. ERT line P1 was acquired first as a "wildcat" test line to see if we could image the tunnel in a relatively accessible area alongside an asphalt path.

ERT line P2 was then acquired after reviewing the maps of the 2004 Urbanavičius report, which indicated the location of the tunnel entrance. Line P2 used a minimum electrode spacing of 10 cm, enabling the shallow subsurface to be imaged in relatively high resolution to depths of up to 1.4 m below the ground surface. As shown in Figure 8b, this line was positioned as close to the circular inner wall of the detention pit as possible, while still maintaining a straight line (the 2D ERT modeling algorithm requires a straight-line geometry).

The processed resistivity cross section for line P2 is displayed in Figure 10a, where the warmer and cooler colors show the most resistive and least resistive materials, respectively. In this model, the circular blue anomaly, representing a zone of resistivities of less than 1000 ohm-m, is interpreted as the tunnel structure, at an approximate depth of 1 m. Above the tunnel anomaly, two distinct soil layers are represented by resistivities less than 1000 ohm-m (the blue discontinuous layer) and another with resistivities generally greater than 3000 ohm-m (the orange to pink colors). The lower resistivity layer is interpreted to be the surficial soil cover, and the higher resistivity layer likely corresponds to dry sands and loosely compacted debris that would have been used to cover the 2004 excavation. Lower resistivity (blue) regions to the sides



Figure 7. Panoramic photos taken over the area of the unmarked pit: (a) looking northeast and (b) looking northwest along ERT line P12.

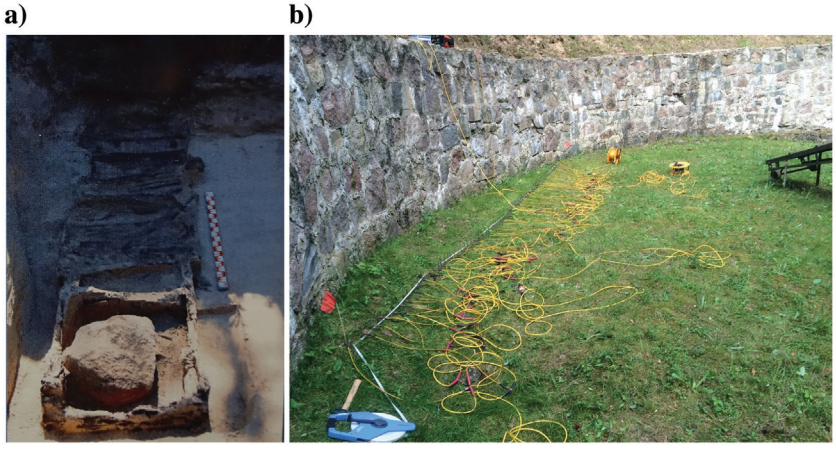


Figure 8. (a) Photo of the uncovered wooden 80 × 95 cm rectangle that formed the entrance to the tunnel, and the wooden framing of the tunnel as it extended back toward the stone walls of the detention pit (Urbanavičius, 2004); the large stone was found within the rectangle and was presumed to be from the original stone foundations of the pit; (b) ERT line P2 (the location is shown in Figure 9), which extended for 8 m between the red pin flags and was centered over the axis of the tunnel, as determined from the excavation plans of Urbanavičius (2004).

Downloaded 12/13/21 to 137.186.57.127. Redistribution subject to SEG license or copyright; see Terms of Use at http://library.seg.org/page/policies/terms
DOI:10.1190/geo2021-0065.1

of the tunnel anomaly are likely influenced by conductive material within the stone foundations, where the ends of the ERT profile are closest to the walls of the pit.

Figure 10b shows the same modeled data plotted in terms of electrical conductivity (the inverse of resistivity). In the conductivity section, the tunnel anomaly corresponds to relatively high conductivities of greater than 1 mS/m (the yellow, orange, and red colors). For clarity, we plotted all of the ERT models from the escape tunnel survey in terms of electrical conductivity. These plots highlight the relatively conductive tunnel anomaly (the yellow, orange, and red colors) relative to the surrounding lower conductivity (the blue colors) loose sand and soil that underlies the site.

If the tunnel was still open, it would be represented as a higher resistivity anomaly because the electrical current would not transmit through an air-filled void. However, the tunnel, as it exists today, has likely been infiltrated with loosely packed sand that has collapsed into the structure. The relatively higher conductivities associated with the tunnel are attributed to a higher moisture content within the disturbed region of the tunnel compared to the surrounding undisturbed and unsaturated sands. Whether they have rotted or are still well preserved, the wooden supports of the tunnel likely retain more moisture from rainfall and snowmelt that has infiltrated the ground than exists in the surrounding well-drained and permeable sands surrounding the structure. Moreover, during the digging of the tunnel, finer grained soil and organic debris with a greater potential to retain moisture were probably tracked and compacted through the tunnel, which could also contribute to the observed higher electrical conductivities.

We note that this "special" situation of a tunnel exhibiting higher electrical conductivities than the surrounding medium would not occur if the tunnel had been excavated through relatively clay-rich soils rather than the relatively dry and uncemented sands and loamy sands present at Ponary (Lietuvos, 1985). ERT line P3 was acquired over the center of the pit, outside the area of the excavated tunnel. This line revealed the same layered subsurface structure as identified on line P2 but no anomalous features that could be correlated to the prison bunker or tunnel.

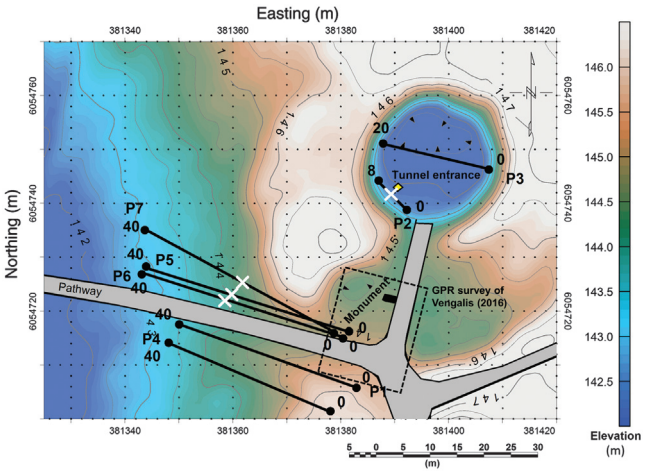


Figure 9. Map showing the layout of the escape tunnel ERT survey lines (the black lines, with numbers indicating the line distance in meters). Elevations are from a LiDAR bare-earth model, displayed with a contour interval of 0.5 m. The yellow square shows the location of the tunnel entrance portal, uncovered by Urbanavičius (2004). The white crosses show the positions of the four high-conductivity anomalies mapped by the ERT lines and interpreted as sections of the tunnel. The rectangular area of the GPR survey of Vengalis (2016) is outlined by the black dashed lines.

Geophysical survey of the tunnel extension

From the few survivor testimonies, the length of the tunnel has been described to be at least 30 m long. Some testimonies suggest that the actual length may have been as long as 40 m (C. Heath, personal communication, 2020). Although there are some discrepancies between accounts, the tunnel may have turned partway along its length to avoid a guard post and a yet-to-be-identified mass grave (e.g., Motke Zaidel described the tunnel being 30 m long and making an abrupt turn to the right after 20 m in length; USHMM, 1979).

To the southwest of the tunnel entrance, a small hill separates the edge of the pit from an area of lower ground where the exit of the tunnel would have been located (Figure 9). Southeast of the hill, in a flat area where a stone monument has been erected (Figure 9), Urbanavičius (2004) opened three trenches, but found no evidence of the tunnel. A 2015 GPR investigation of the flat area around the monument clearly imaged reflections from subhorizontal sedimentary layering, to depths of at least 7 m, but it found no evidence of the escape tunnel in this area (Figure 9; Vengalis, 2016). The crest of the hill is at least 6 m higher than where the tunnel entrance was uncovered in 2004. Consequently, Urbanavičius (2004) may have avoided trenching in this area because the depth to the tunnel may have made opening a trench here impractical. Similarly, any ERT profiles crossing the hill were unlikely to detect and resolve a 65 × 55 cm tunnel at depths greater than 5 m, and the variable topography is difficult to model accurately using available processing algorithms. For these reasons, we focused further investigation

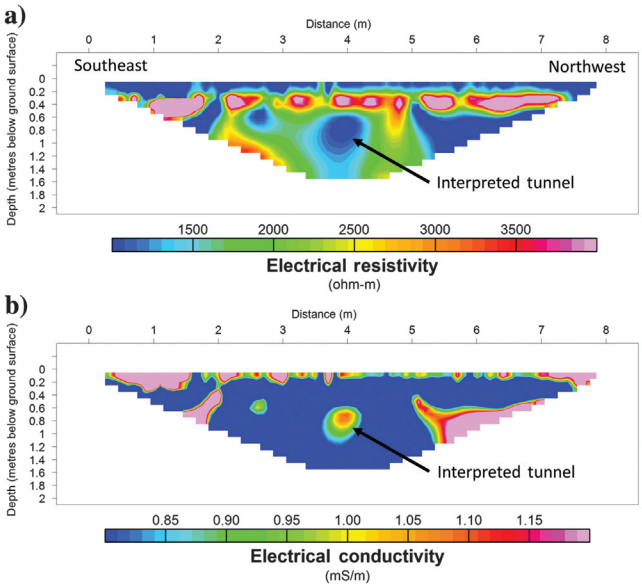


Figure 10. ERT (a) resistivity and (b) conductivity models produced from ERT line P2, over the excavated tunnel entrance (the location is shown in Figure 9). The tunnel entrance coincides with a low-resistivity (or high-conductivity) circular anomaly approximately 80 cm below the ground surface. The layer of high-resistivity material (the pink blobs) above the tunnel entrance anomaly is interpreted as sand and potential stone debris, from the pit walls, within the shallow fill.

Downloaded 12/13/21 to 137.186.57.127. Redistribution subject to SEG license or copyright; see Terms of Use at http://library.seg.org/page/policies/terms
DOI:10.1190/geo2021-0065.1

in the lower elevation areas to the southwest of the hill, where the tunnel would have been closer to the ground surface, and where having a tunnel end along with a tunnel entrance would explicitly confirm a complete tunnel (see the ERT profile locations P1 and P4-P7 in Figure 9). ERT profiles P1 and P4-P7 were all acquired using a minimum electrode spacing of 0.5 m, providing a reliable depth of investigation of approximately 5 mbgs.

The results from the initial profile P1, on the south side of the asphalt pathway, revealed layering within the soil profile, but they did not show a distinctive conductive anomaly comparable to that imaged over the tunnel near the entrance portal. Profile P4 was acquired to the south of P1, over two small depressions that, at the time, were speculated to have been possible remnants of a tunnel exit, although no significant anomalies could be correlated to these features (Figure 9; the cross sections are not shown). The depressions transected by line P4 were located more than 40 m from the tunnel entrance and are more likely associated with reconstruction of the site after the war.

The final stage of the investigation targeted the low area immediately to the north of the paved pathway, at the base of the hill (lines P5, P6, and P7 in Figure 9). Figure 11 displays the ERT conductivity cross sections from these three profiles, with the profile plotted furthest from the detention pit (P6) plotted in the top panel and the profile closest to the pit (P7) plotted in the lowest panel. Each cross section has been corrected for changes in topography (the southeastern end of each profile is approximately 2 m higher than the northwestern end) and has been plotted in terms of elevation (in meters above sea level [masl]), rather than depth.

On all three profiles shown in Figure 11, relatively high conductivity anomalies observed at depths between 2.2 and 3.0 m are interpreted as the remnants of the tunnel. Between the two outermost profiles, P6 and P7, over a distance of 4.5 m, small changes in depth to the anomalies occur. This variability in the depth of the tunnel is attributed to changes in the ground surface elevation along each ERT line and, to a lesser degree, the potential shallowing of the tunnel as it approached the likely exit point. Nevertheless, the tops of the anomalies on lines P5, P6, and P7 all occur at a relatively uniform elevation of 142 masl. Similarly, the elevation of the top of the tunnel entrance anomaly identified on line P2 is approximately 142 masl (the ground surface along line P2 is at an elevation of approximately 142.5 masl; Figure 9).

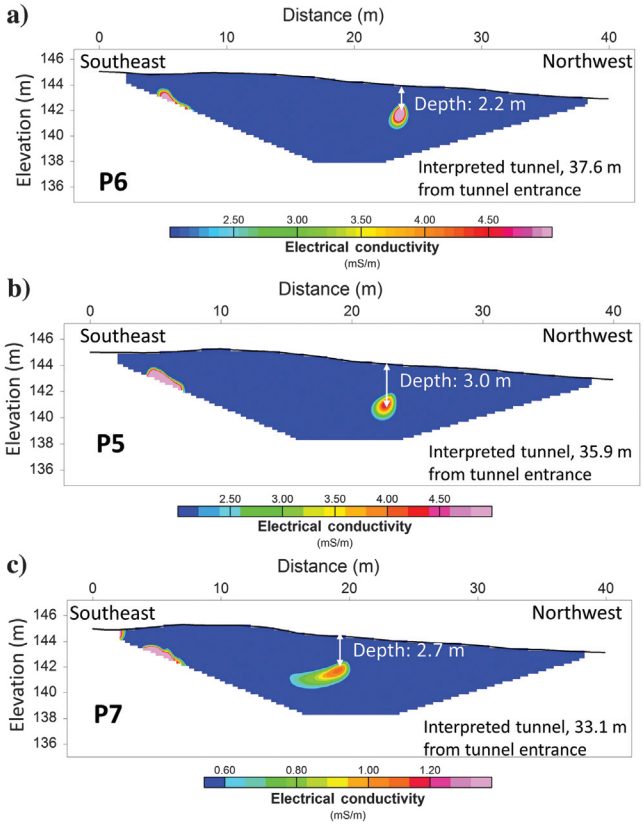


Figure 11. ERT conductivity cross sections from ERT lines (a) P6, (b) P5, and (c) P7. The distinctive relatively high conductivity anomalies are interpreted as parts of the tunnel. See Figure 9 for the line locations.

Discussion of the tunnel survey results

As was observed at the tunnel entrance by Urbanavičius (2004), we expect that the conductivity anomalies are partially associated

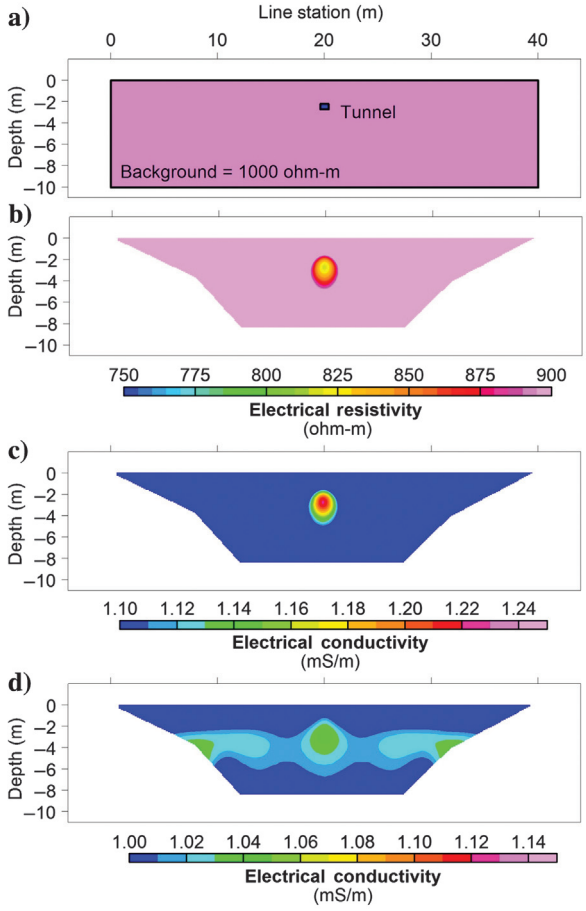


Figure 12. Results of the synthetic modeling of the tunnel anomaly. (a) A 2D model showing the theoretical tunnel geometry, (b) the resulting resistivity model generated from the synthetic data produced from the model shown in (a) with tunnel resistivity of 100 ohm-m, (c) the same as for (b) but displayed in terms of conductivity, and (d) the resulting conductivity model from the synthetic data produced from the model shown in (a), but with the tunnel resistivity set to 500 ohm-m.

Downloaded 12/13/21 to 137.186.57.127. Redistribution subject to SEG license or copyright; see Terms of Use at http://library.seg.org/page/policies/terms
DOI:10.1190/geo2021-0065.1

with the timber supports of the tunnel. It is possible that other materials or objects may have been left inside the tunnel that would also contribute to the source of the conductivity anomalies. We expect that the tunnel has either collapsed or is partially infilled with material causing elevated conductivities relative to background values (e.g., finer-grained sediment or organic soil tracked into the tunnel). The tunnel would not be open because an air-filled void would exhibit higher resistivities than the background material.

To demonstrate the resistivity contrast required to generate the anomalies imaged on the profiles shown in Figure 11, we constructed synthetic models for different scenarios, calculated the expected apparent resistivity data from the models, and generated inverted resistivity cross sections for each model. Using the commercially available RES2DMOD resistivity modeling package, we constructed models with a uniform background resistivity of 1000 ohm-m and a 70 cm wide and 50 cm high rectangular tunnel, centered at a depth of 2.5 mbgs, which is comparable to the depth of the anomalies imaged in Figure 11 (the model geometry is shown in Figure 12a). A background value of 1000 ohm-m was deemed to be representative of the background resistivity values measured for lines P5, P6, and P7. Synthetic apparent resistivity data were generated from the models using a multiple-gradient array sequence comparable to the measurement arrays used for lines P5, P6, and P7, and with 81 electrode positions, spaced at 0.5 m intervals. Gaussian noise of 2% was added to the exported data.

Figure 12b shows the inverted resistivity model for a tunnel body with a uniform resistivity of 100 ohm-m. The corresponding conductivity section shown in Figure 12c shows that this resistivity contrast produces a close match to the field data sections shown in Figure 11. Figure 12d shows the equivalent model result but for a tunnel body with a resistivity of 500 ohm-m. The lesser resistivity contrast for the model result shown in Figure 12d is not sufficient for the tunnel to be resolved effectively. Therefore, the inverted resistivity models for lines P5, P6, and P7 are likely imaging a tunnel body that has bulk resistivities roughly an order of magnitude lower than the resistivities of the surrounding unsaturated sandy sediments.

We note that all three anomalies associated with the escape tunnel occur over a relatively constant elevation of approximately 142 masl, very similar to the elevation of the tunnel at the entrance (approximately 142 masl). The narrow range of elevations implies that the tunnel would have had only a very slight gradient from the entrance toward the tunnel exit. A tunnel constructed at a steeper angle may have required more complicated reinforcement to prevent the tunnel collapsing. Although the true nature of the linear anomaly identified from ERT profiles P5, P6, and P7 cannot be confirmed without excavation of the target, the depth, dimensions, and orientation of the linear feature fit with the description of the tunnel entrance excavated in 2004 and with the descriptions from survivor testimony.

It is understood that 12 of the Leichenkommando survived the escape attempt on 15 April 1944, whereas an unconfirmed number were killed either after exiting the tunnel (shot by guards or wounded by land mines) or perished inside the tunnel. The details of the escape are difficult to piece together from the disparate accounts from the survivors, and some key details differ between accounts (e.g., the 1979 interviews with survivors Motke Zaidel and Itzak Dugin for the *Shoah* film in USHMM [1979]; the account of Yuri Farber in Ehrenburg and Grossman [1986], first published in 1946; and the autobiographical account of Shlomo Gol in Gol [1954]). However, at least one account describes how pliers, salvaged from some of the corpses exhumed from the mass graves, were used to cut through a barbed wire fence. After escaping, some of the survivors, including Shlomo Gol, made contact with partisan resistance fighters and, in July 1944, helped liberate Vilnius from German occupation (Gol, 1954).

Based on survivor testimonies of a tunnel that was potentially as long as 40 m, the geophysically mapped tunnel segment would be close to the exit of the tunnel where survivors recall breaking a hole through the roof of the tunnel once they had encountered the root zone of the trees (testimony of Motke Zaidel and Itzak Dugin for the *Shoah* film in USHMM, 1979). The tunnel would be considerably deeper at distances closer to the detention pit, and shallower at distances closer to the exit. Because the tunnel would be more difficult for archaeologists to excavate at greater depths, and at shallower depths it is more likely to have collapsed or been removed by post-World War II reconstruction of the site, the segment mapped using ERT on the north side of the asphalt path would be the ideal location to excavate an archaeological trench to expose the structure. Prior to any archaeological excavation, it would be worthwhile to acquire additional ERT profiles to further delineate the extents of the interpreted tunnel segment.

CONCLUSION

The results of the 2016 geophysical investigation contribute two important new details to the history of the Ponary extermination site: (1) the existence and delineation of a large unmarked mass grave and (2) the existence and delineation of a segment of the escape tunnel constructed and used by the Leichenkommando in 1944. The mass grave was confirmed using a combination of results from ERT, GPR, and the LiDAR topography survey. Based on these results, we determined that the circular pit had a diameter of approximately 25 m and it extended to a depth of approximately 4 m. The contents of the pit, whether ash or intact human remains, cannot be distinguished, but the resistivity measurements show a significant contrast with the surrounding sandy soil and sediments, clearly indicating an infilled pit.

The entrance to the escape tunnel from the detention pit, which was excavated in 2004, was imaged using ERT, and corresponded with a high-conductivity (or low-resistivity) anomaly. The cause of the higher conductivities is attributed to the higher moisture content within the tunnel structure than in the surrounding, well-drained sandy sediments. A 4.5 m segment of the tunnel was mapped on three ERT profiles located between 33.1 and 37.6 m from the tunnel entrance. This segment of the tunnel is associated with small, relatively high conductivity anomalies that are centered at depths of between 2.2 and 3.0 m below the ground surface. The results of the 2016 geophysical investigation will be used to demarcate the areas of the suspected mass grave and the escape tunnel so that they can be appropriately memorialized and protected from subsequent development at the Ponary extermination site.

ACKNOWLEDGMENTS

We wish to acknowledge funding provided by BGC Engineering Inc., the US Commission for the Preservation of America's Heritage Abroad, the US Embassy in Lithuania, the University of Hartford's Maurice Greenberg Center for Judaic Studies, the University

Downloaded 12/13/21 to 137.186.57.127. Redistribution subject to SEG license or copyright; see Terms of Use at http://library.seg.org/page/policies/terms
DOI:10.1190/geo2021-0065.1

of Wisconsin–Eau Claire, Duquesne University, the Antiquities Authority of Israel, the filming and sponsors of the PBS NOVA Science series, the Student Blugold Commitment funds at the University of Wisconsin–Eau Claire — in particular the International Fellows Program for Research, Service, and Creative Activity as well as Student Differential Tuition funds through the University of Wisconsin–Eau Claire Diversity Mentoring program, and the Jewish Community of Lithuania. Access to the site was granted by the Vilna Gaon State Jewish Museum, and we thank M. Šikšnianas for the guidance and assistance accessing historical information. J. Francke and D. Goodman assisted with processing of the GPR data. The use of the ERT system and all associated geophysical, drone, and mapping equipment were donated by Paul Bauman Geophysics Ltd. This study complements additional geophysical site investigations of Holocaust sites in Lithuania and Poland that were undertaken as part of a research project funded by the SEG Geoscientists Without Borders program.

DATA AND MATERIALS AVAILABILITY

Data associated with this research are available and can be obtained by contacting the corresponding author.

REFERENCES

Abate, D., C. Sturdy Colls, N. Moyssi, D. Karsili, M. Faka, A. Anilir, and S. Manolis, 2019, Optimizing search strategies in mass grave location through the combination of digital technologies: Forensic Science International: Synergy, **1**, 95–107, doi: 10.1016/j.fsisyn.2019.05.002.

Arsenault, C., 2019, 1 in 5 Canadian youths not sure what happened in the Holocaust, survey suggests, CBC News, https://www.cbc.ca/news/canada/canada-holocaust-survey-remembrance-1.4994602, accessed 27 January 2019.

Barone, P. M., C. Ferrara, E. Pettinelli, and A. Fazzari, 2016, Forensic geophysics: How the GPR technique can help with forensic investigations, *in* H. Kars and L. van den Eijkel, eds., Soil in criminal and environmental forensics: Springer, 213–227.

Bauman, P. D., A. McClymont, J. Seligman, R. Freund, H. Jol, P. Reeder, C. Slater, and C. Miazga, 2020, Geophysical investigations at Holocaust sites in Lithuania and Warsaw — A multimethod geoscience approach to mapping mass graves and associated sites of atrocity crimes, Technical report for geoscientists without borders, 307074-01588-GP-REP-0001, https://seg.org/About-SEG/Geoscientists-Without-Borders/Projects/detail/lithuania, accessed 26 February 2020.

Bevan, B. W., 1991, The search for graves: Geophysics, **56**, 1310–1319, doi: 10.1190/1.1443152.

Bubnys, A., 2004, Holocaust in Lithuania: An outline of the major stages and their results, *in* S. Schreiner, L. Donskis, and A. Nikzentaitis, eds., The vanished world of Lithuanian Jews: Rodopi, 218–219.

Burds, L. T., J. D. Beck, R. J. Mataitis, H. M. Jol, R. A. Freund, A. F. McClymont, and P. Bauman, 2018, Holocaust archaeology: Using ground penetrating radar to locate a Jewish mass grave in Kaunas, Lithuania: Proceedings of the 17th International Conference on Ground Penetrating Radar.

Chan, P., 2019, Red stars and yellow stars: The Soviet investigation of Klooga Concentration Camp: Holocaust and Genocide Studies, **33**, 197–224, doi: 10.1093/hgs/dcz022.

Cheetham, P., 2005, Forensic geophysical survey, *in* J. Hunter and M. Cox, eds., Forensic archaeology: Advances in theory and practice: Routledge, 62–95.

Dahlin, T., V. Leroux, and J. Nissen, 2002, Measuring techniques in induced polarisation imaging: Journal of Applied Geophysics, **50**, 279–298, doi: 10.1016/S0926-9851(02)00148-9.

Dahlin, T., and B. Zhou, 2004, A numerical comparison of 2D resistivity imaging with 10 electrode arrays: Geophysical Prospection, **52**, 379–398, doi: 10.1111/j.1365-2478.2004.00423.x.

Dahlin, T., and B. Zhou, 2006, Multiple-gradient array measurements for multichannel 2D resistivity imaging: Near Surface Geophysics, **4**, 113–123, doi: 10.3997/1873-0604.2005037.

Ehrenburg, I., and V. Grossman, 1986, The black book: The ruthless murder of Jews by German-Fascist invaders throughout the temporarily-occupied regions of the Soviet union and in the death camps of 1942–1945 (English and Russian Edition): Holocaust Library, 595.

Fenning, P. J., and L. J. Donnelly, 2003, Geophysical techniques for forensic investigation: Geological Society of London Special Publications, **232**, 11–20, doi: 10.1144/GSL.SP.2004.232.01.03.

Freund, R., 2019, The archaeology of the Holocaust — Vilna, Rhodes, and escape tunnels: Rowman & Littlefield.

Gol, S., 1954, Escape from Ponar, *in* Y. Zuckerman and M. Bassok, eds., The book of the Ghetto Wars: Tel Aviv, Hakibutz HaMeukhad, 566–570.

Hammerstedt, S. W., and A. L. Regnier, 2019, Searching for graves from the 1921 Tulsa Race Massacre: Geophysical survey of Oaklawn Cemetery, the Canes, and Newblock Park: Oklahoma Archeological Survey Research Series 5.

Jones, G., 2008, Geophysical mapping of historic cemeteries: Technical Briefs in Historical Archaeology, **3**, 25–38.

Lietuvos, 1985, Lietuvos TSR dirvozemio zemelapis M 1:300000, RZPI, Vilnius, 215.

Loke, M. H., and R. D. Barker, 1996, Rapid least-squares inversion of apparent resistivity pseudosections using a quasi-Newton method: Geophysical Prospecting, **44**, 131–152, doi: 10.1111/j.1365-2478.1996.tb00142.x.

Noel, M., and B. Xu, 1991, Archaeological investigation by electrical resistivity tomography: A preliminary study: Geophysical Journal International, **107**, 95–102, doi: 10.1111/j.1365-246X.1991.tb01159.x.

Powell, K., 2004, Detecting buried human remains using near-surface geophysical instruments: Exploration Geophysics, **35**, 88–92, doi: 10.1071/EG04088.

Ramgopal, K., 2020, Survey finds 'shocking' lack of Holocaust knowledge among millennials and Gen Z: NB News, https://www.nbcnews.com/news/world/survey-finds-shocking-lack-holocaust-knowledge-among-millennials-gen-z-n1240031, accessed 16 September 2020.

Renshaw, L., 2013, The exhumation of civilian victims of conflict and human rights abuses, *in* L. N. Stutz and S. Tarlow, eds., The Oxford handbook of the archaeology of death and burial: Oxford University Press.

Rozycki, S., R. Zaplata, J. Karczewski, A. Ossowski, and J. Tomczyk, 2020, Integrated archaeological research — Archival resources, surveys, geophysical prospections and excavation approach at an execution and burial site: The German Nazi labour camp in Treblinka: Geosciences, **10,** 336, doi: 10.3390/geosciences10090336.

Sakowicz, K., 2005, Ponary diary, 1941–1943: A bystanders account of a mass murder, Y. Arad, ed.: Yale University Press.

Schultz, J. J., 2012, The application of ground-penetrating radar for forensic grave detection, *in* D. Dirkmaat, ed., A companion to forensic anthropology: Blackwell Publishing Ltd., 85–100.

Seligman, J., P. Bauman, R. Freund, H. Jol, A. McClymont, and P. Reeder, 2020, Mapping Ponar (Paneriai): A reassessment: Human Remains and Violence, **6**, 15–39, doi: 10.7227/HRV.6.1.3.

Snyder, T., 2010, Bloodlands — Europe between Hitler and Stalin: Basic Books.

Sturdy Colls, C., 2015a, Holocaust archaeologies: Approaches and future directions: Springer.

Sturdy Colls, C., 2015b, Learning from the present to understand the past: Forensics and archaeological approaches to sites of the Holocaust, *in* T. Lutz, D. Silberklang, P. Trojanski, J. Wetzel, and M. Bistrovic, eds., Killing sites — Research and remembrance: Metropol Verlag, 61–78.

Tomkiewicz, M., 2008, Zbrodnia w Ponarach 1941–1944 [The Ponary Massacre 1941–1944]: Warsaw.

Urbanavičius, V., 2004, Panerių memorialas — Buvusio kalėjimo 2004 m. tyrimų ataskaita. [Paneriai Memorial — Former Prison 2004 Investigations Report], Archaeological report, translated to English from Lithuanian, stored in Manuscript Department at the Lithuania Institute of History (F.1, b.4416), 50.

USHMM, 1979, Claude Lanzmann Shoah Collection Interview of September 18-19, 1979, with Motke Zaidel and Itzak Dugim, translated into English from unedited footage by Anna Dhaliwal in 2008, United States Holocaust Museum Film Accession Number 1996.166, https://collections.ushmm.org, accessed 12 July 2016.

USHMM, 1995, Forensic experts official report of the Soviet Extraordinary State Commission, United States Holocaust Memorial Museum archive, RG-22.002M, f.7021, op. 116, d. 1,ii. 0085-0100,0183-84, Original archive reference GARF 94-1-7021, 11572, State Archive of the Russian Federation (GARF).

USHMM, 2020, United States Holocaust Memorial Museum, Holocaust Encyclopedia, https://encyclopedia.ushmm.org/content/en/article/lithuania, accessed 15 January 2021.

Van der Laarse, R., 2013, Archaeology of memory — Europe's Holocaust dissonances in east and west, *in* D. Callebout, J. Marik, and J. Marikova-Kubkova, eds., Heritage reinvents Europe, Proceedings of the Internationale Conference Ename, Europae Archaeologiae Consilium/Archaeolingua.

Vengalis, R., 2016, Panerių žudynių vietos ir kapų žvalgymai geofizikiniais metodais [Geophysical Survey in Paneriai Massacre and Grave Site], *in* G. Zabiela, ed., Archeologiniai tyrinėjimai Lietuvoje 2015 metais: Society of the Lithuanian Archaeology, 527–531.

Biographies and photographs of the authors are not available.